Electronic Supplementary Information (ESI) for

High-performance sensing, breathable, and biodegradable integrated wearable sweat biosensors for wireless glucose early warning system

He Zhao, [a] *Ling Zhang,* [*a] *Tianbo Deng* [a] *and Chunzhong Li* [*a]

a. Key Laboratory for Ultrafine Materials of Ministry of Education, Frontiers Science Center for Materiobiology and Dynamic Chemistry, School of Materials Science and Engineering, East China University of Science & Technology, Shanghai 200237, China. E-mail: zlingzi@ecust.edu.cn, czli@ecust.edu.cn.

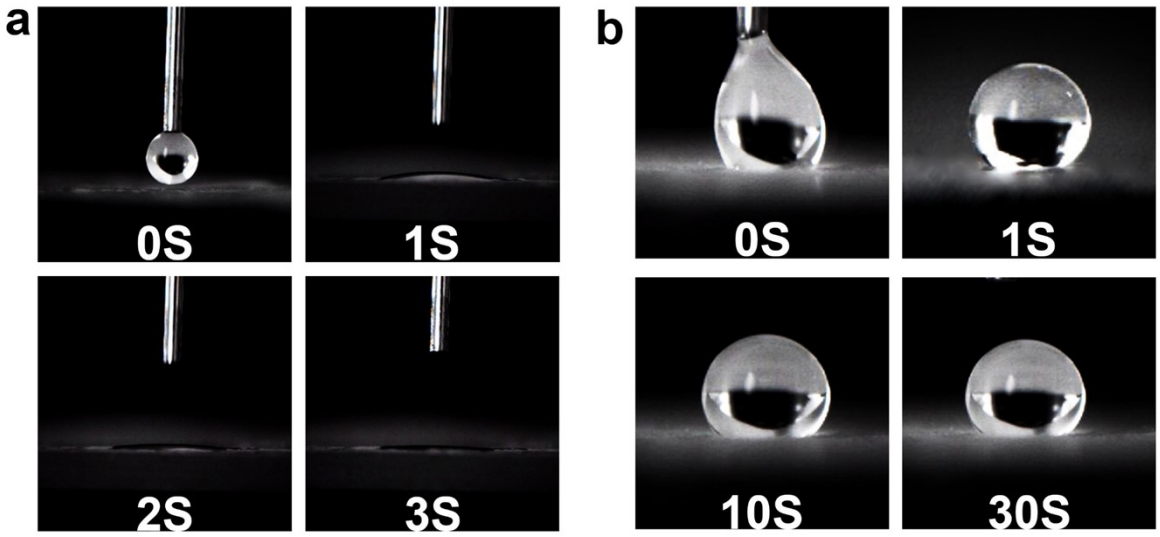

Fig. S1 The images of the water contact angle of (a) the hydrophilic patterned nanofibers and (b) the PCL nanofibers.

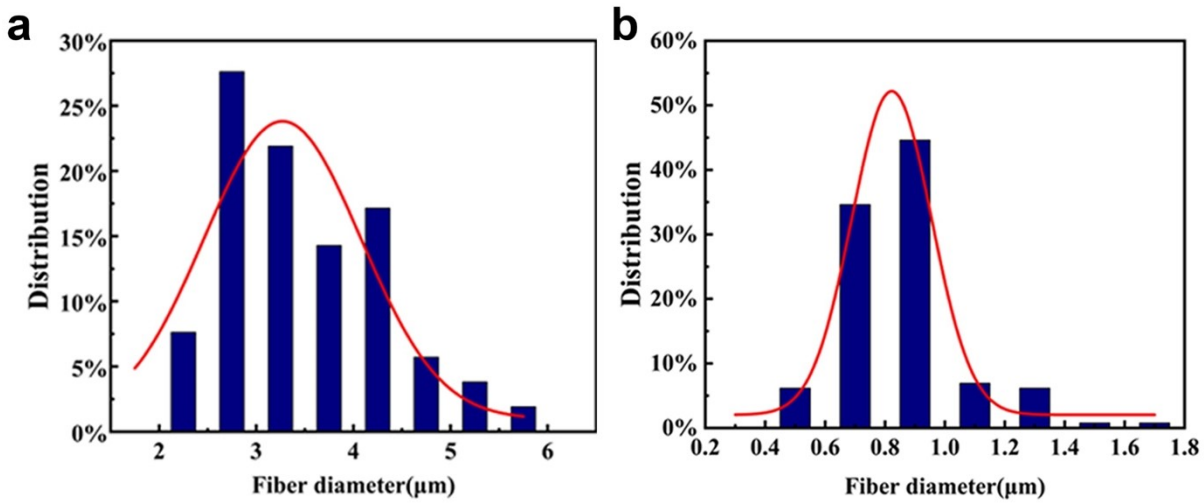

Fig. S2 The average diameter of (a) the PCL nanofibers, and (b) the hydrophilic patterned nanofibers.

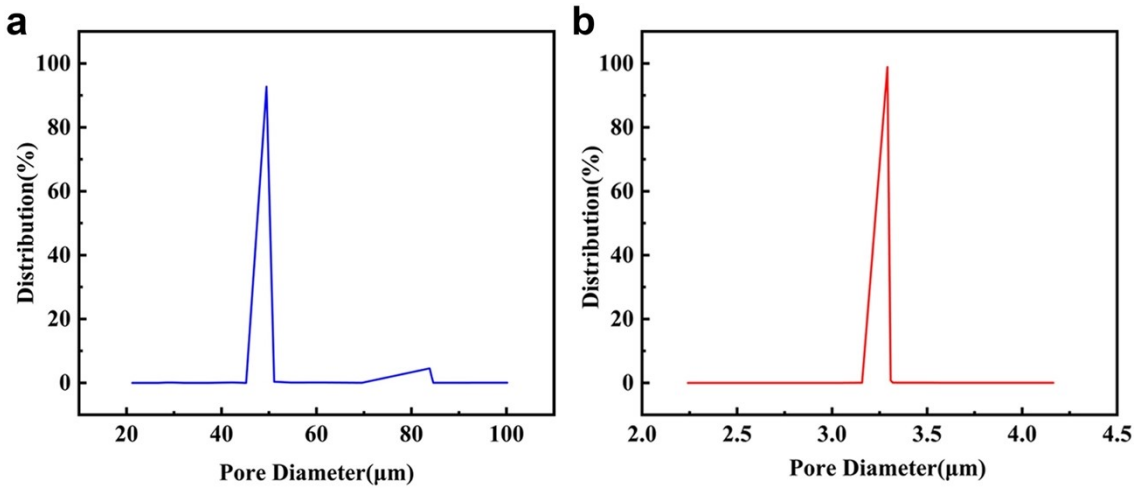

Fig. S3 Aperture distribution of (a) the PCL nanofibers and (b) the hydrophilic patterned nanofibers.

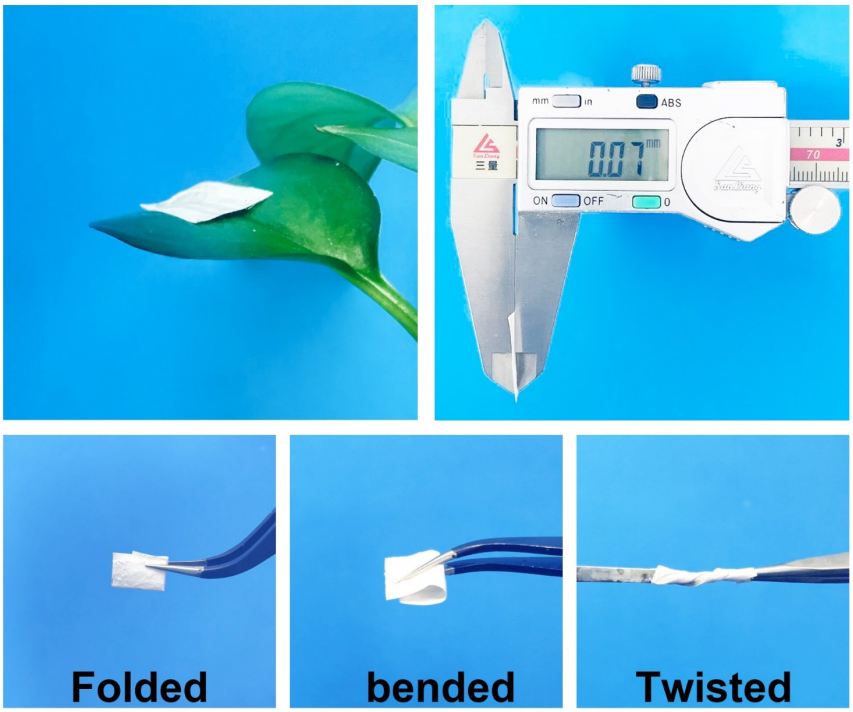

Fig. S4 Photograph images of the wearable glucose sensor with a total thickness of 70 μm placed on a leaf. Optical images demonstrate the excellent flexibility of the wearable glucose sensor.

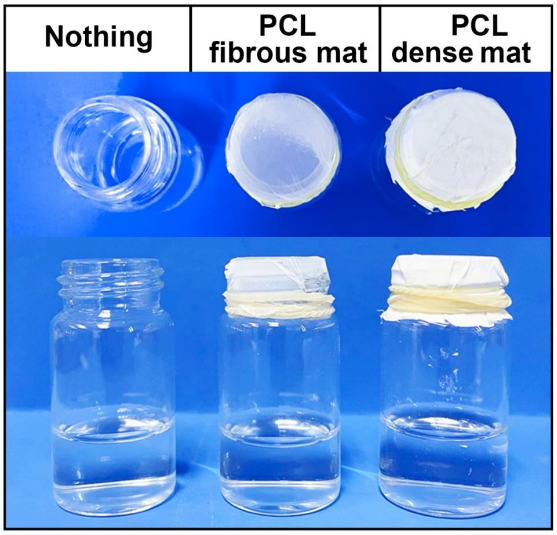

Fig. S5 Optical photographs of the breathability test process at room temperature.

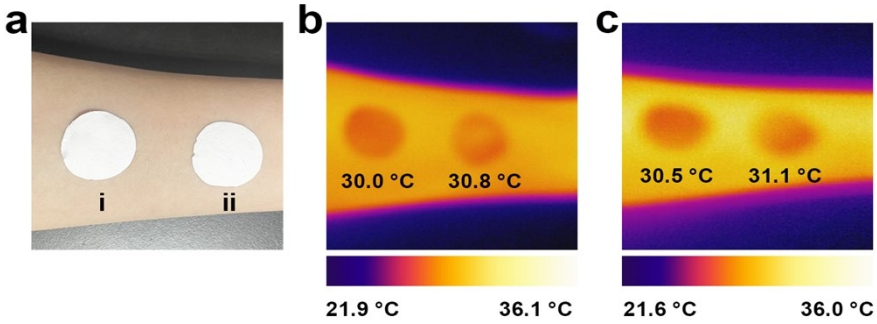

i) Hydrophobic-hydrophilic PCL fibrous mat

ii) Hydrophobic-hydrophobic PCL fibrous mat

Fig. S6 Optical (a) and infrared photos of the hydrophobic-hydrophilic and hydrophobic-hydrophobic fibrous mats on the skin before (b) and after sweating (c).

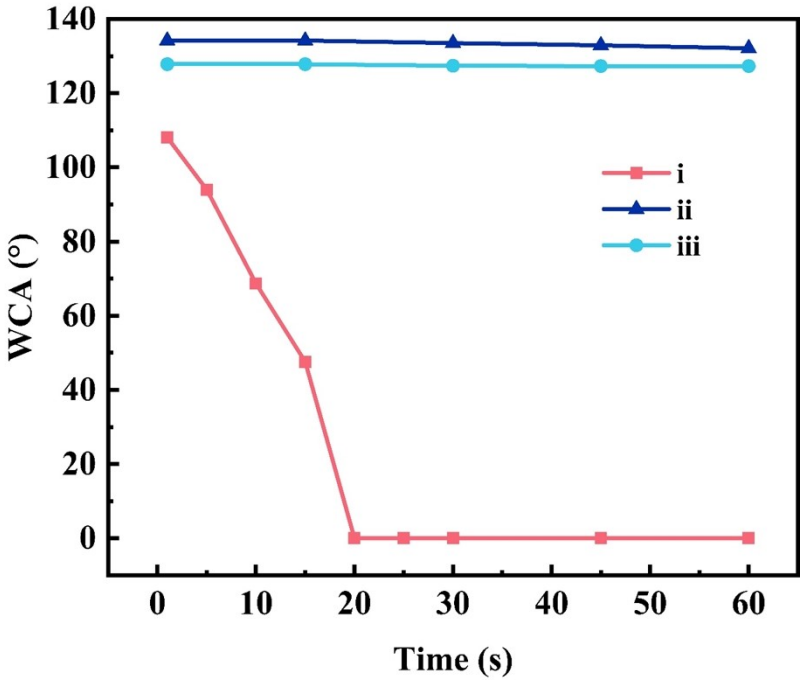

Fig. S7 Dynamic water contact angles of the i) hydrophilic-hydrophobic fibrous mats, ii) hydrophobic-hydrophobic fibrous mats with a porosity gradient, and iii) hydrophilic-hydrophobic fibrous mats with the same pore size.

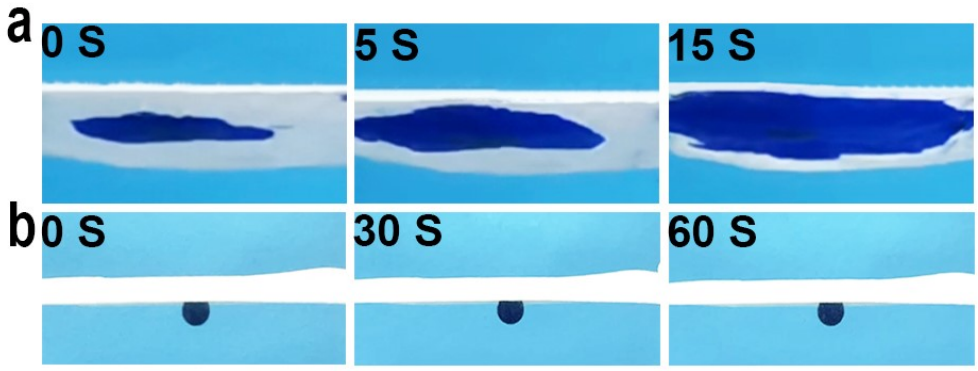

Fig. S8 (a) 10 μL methylene blue drops were added below the hydrophobic-hydrophilic fibrous mat with the porosity gradient on the hydrophilic side. (b) 10 μL methylene blue drops were added below the hydrophobic-hydrophobic fibrous mat with the porosity gradient on the hydrophobic side.

A sweat-generation system was used to simulate the sweating process of the skin and characterize the Sweat collection capability of the devices (Fig. S7). The sweat was generated at a different rate through the syringe pump, which was then collected by the fibrous mat. The sweat collection efficiency was calculated by:[1]

$$\text{Sweat collection efficiency} = \frac{m_s}{RST\rho}$$

Where R, S, T, and ρ were the injection rate of sweat, the sensing area, test time, and density of sweat, respectively; m_s was the mass of the collected sweat in the sensing area. The tests were repeated at least three times.

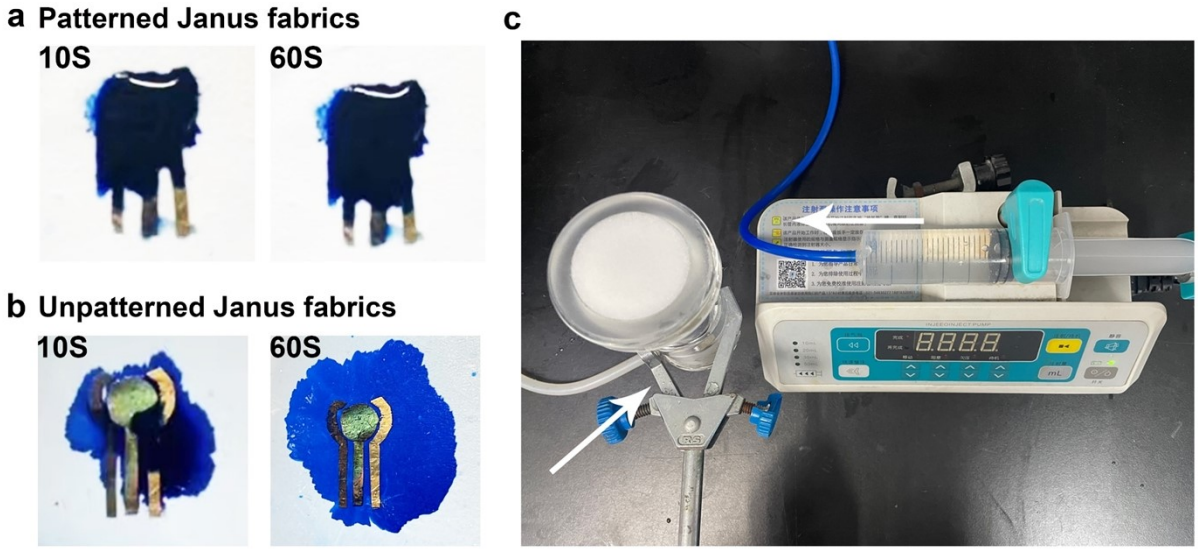

Fig. S9 Digital photos show the biosensor based on (a) patterned and (b) unpatterned Janus fabrics for the sweat collection process. (c) Experimental setup of the sweat-generation system.

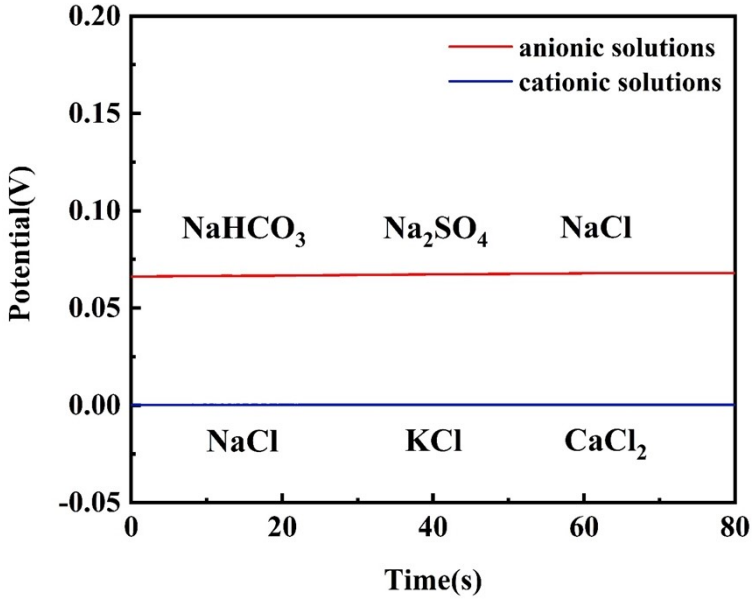

Fig. S10 The stability of flexible reference electrodes in solutions containing 50 mM NaCl and 10 mM of different cationic and anionic solutions.

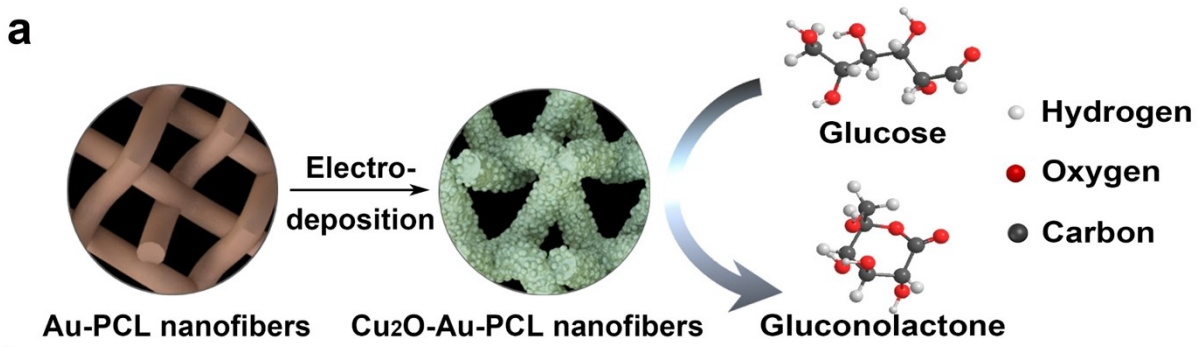

b

$$Cu_2O + 3H_2O \rightarrow 2Cu(OH)_2 + H_2$$

$$Cu(OH)_2 \rightarrow CuO + H_2O$$

$$CuO + OH^- \rightarrow CuO(OH) + e^-$$

$$CuO(OH) + e^- + \text{glucose} \rightarrow CuO + OH^- + \text{gluconolactone}$$

Fig. S11 (a) The schematic diagram for the fabrication of glucose-sensing fibrous electrodes. (b) The schematic diagram of reaction mechanism.

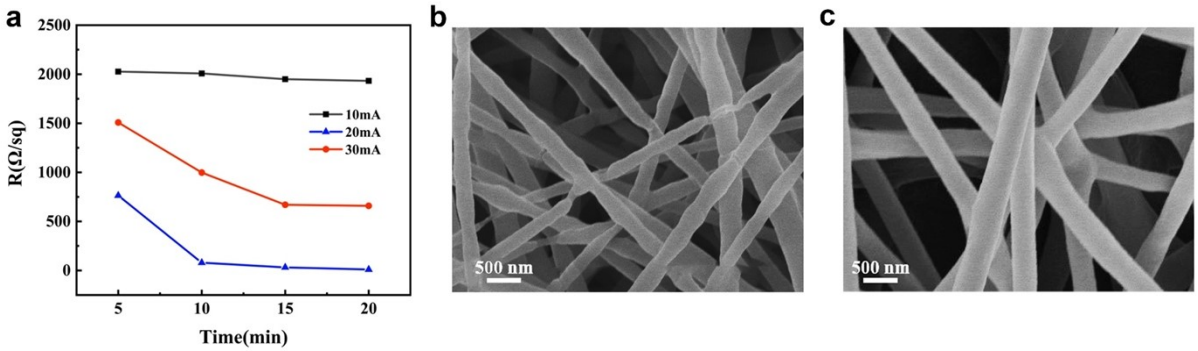

Fig. S12 (a) The sheet resistance of the Au-PCL nanofibers at different times and operating currents. SEM images of Au-PCL nanofibers at an operating current of (b)30 mA and (c) 20 mA (sputtering time: 20 minutes).

The CVs at different scan rates of the glucose sensing fibrous electrode in PBS solution in the presence of 3 μM glucose solution over a voltage range from -0.2 to 0.8 V (versus Ag/AgCl) were recorded, as shown in Fig. S11a. The increase in scan rate affects the position of the redox peak and redox peak current. The cathodic and anodic current densities positively correlated with the scan rate, while the cathodic peak potentials shifted negatively. These indicated a quasi-reversible electron transfer reaction process in the glucose electrochemical reaction. The redox's peak current densities were proportional to the scan rates' square root. Direct linearity between the square root of the scan rates and the peak current (Ip) densities was obtained in the range from 10 to 200 mV s^{-1}. Fig. S11b shows the linearly fitted curve, indicating that the electrochemical oxidation of glucose on the electrode is a typical diffusion-controlled electrochemical process. Furthermore, to prove the potentiality of glucose detection using the Cu_2O-Au-PCL nanofibers as a non-enzymatic biosensor, the electrocatalytic activity was further assessed in diverse glucose concentrations from 0.02 to 0.10 mM by CV curves measurements at a scan rate of 100 mVs^{-1}. Fig. S11c shows that the anodic current increases with glucose concentration upon the stepped glucose addition, whereas the cathodic peak currents decrease. Hence, these results strongly indicate that Cu_2O has good electrocatalytic activity toward glucose oxidation.

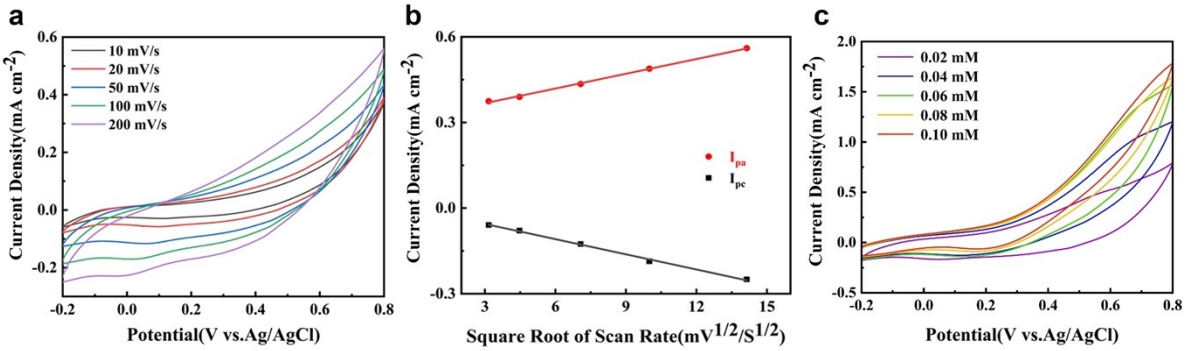

Fig. S13 (a) CV curves of Cu_2O-Au-PCL nanofibers at different scan rates from 10 to 200 mV s^{-1}. (b) The linear calibration plot of the peak current densities versus the square root of scan rate extracted from (a). (c) CV curves of the Cu_2O-Au-PCL nanofibers at a scan rate of 100 mV s^{-1} in different glucose solutions (ranging from 0.02 to 0.10 mM).

The limit of detection (LOD) of the electrode towards glucose can be calculated as the following formula based on a signal-to-noise ratio of 3 (S/N):

$$\text{LOD}=\frac{3S_b}{S}$$

where S_b is the standard deviation of the background current and S is the slope of the linear fitting curve.

An increase in glucose concentration leads to a decrease in the slope of the fitted plot because the electrochemical oxidation of glucose is influenced by the glucose concentration and the catalyst surface active sites. As the glucose concentration increases, the number of available surface-active sites decreases and therefore the increase in the current rate slows down.[2]

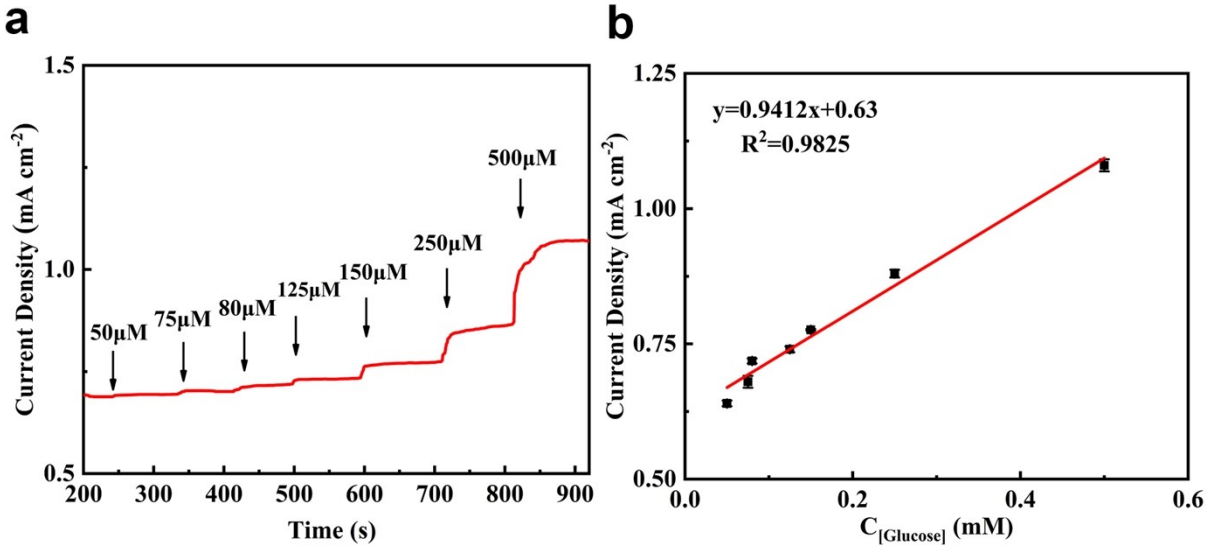

Fig. S14 (a) Amperometric response with successive additions of glucose. (b) Linear calibration curve of the current density versus the concentration of glucose, calculated from the amperometric response curves. (All the data points show excellent reproducibility with relative standard deviations of 0.52%, 1.09%, 0.46%, 0.54%, 0.16%, 0.72%, and 1.11% (N=4).)

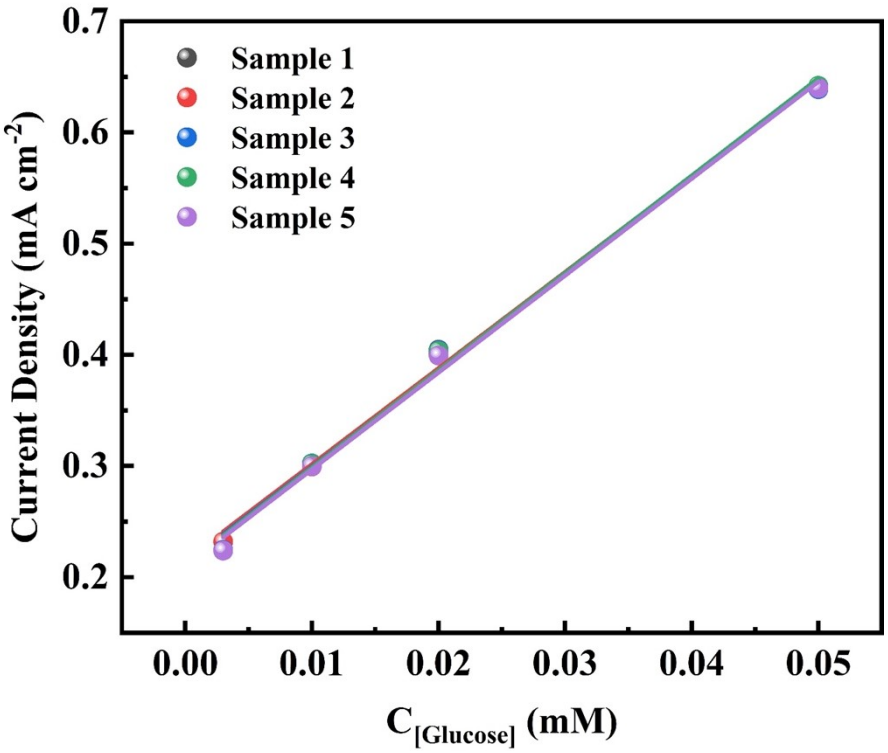

Fig. S15 The reproducibility of the Cu_2O-Au-PCL nanofibers in response to glucose.

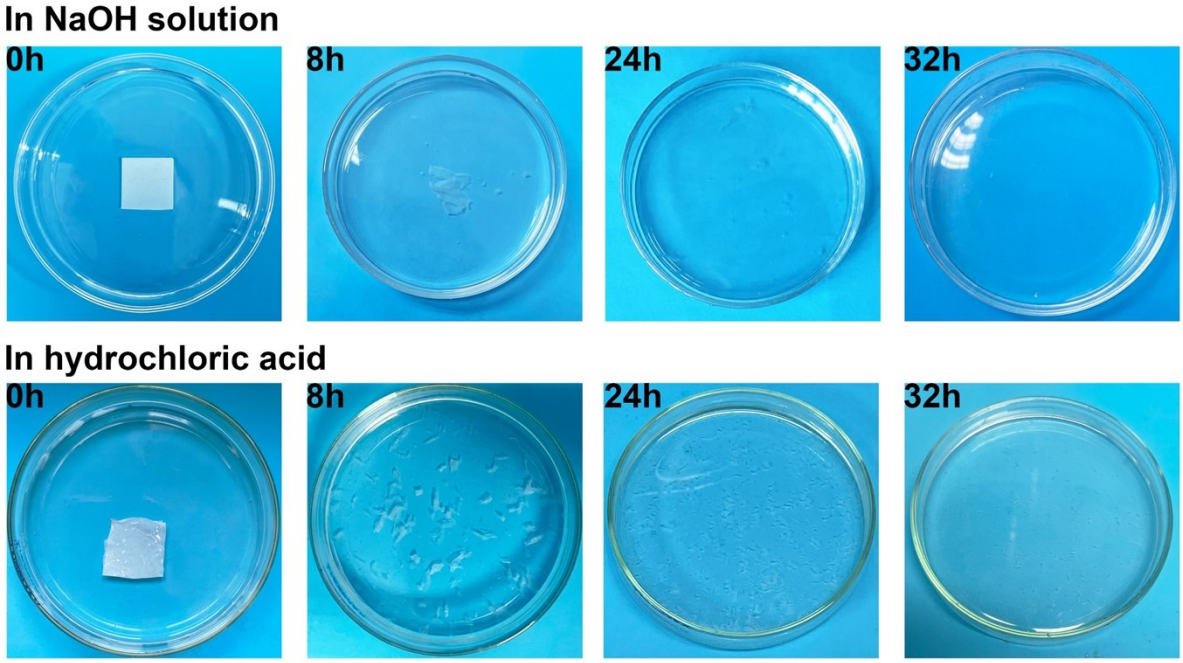

Fig. S16 Sequential photographs of the in vitro degradation of PCL fibrous mats in NaOH solution and hydrochloric acid.

Supplementary Note 1

X-ray diffraction (XRD) analysis on the Cu_2O-Au-PCL nanofibers and PCL nanofibers is shown in Fig. 2j. In the XRD pattern of the Cu_2O-Au-PCL nanofibers, four new peaks matched well with the (111), (200), (220), (311) of Cu_2O (JCPDS No.05-0667), respectively.[3, 4] The Cu 2p X-ray photoelectron spectroscopy (XPS) spectrum exhibited the core-level Cu 2p1/2, and Cu 2p3/2 was fitted into two major peaks at 952.2 and 932.4 eV (Fig. 2k), which was in good agreement with previous reports for Cu_2O.[5] The above results confirmed that Cu_2O was successfully prepared. Meanwhile, the peaks of Cu 2p1/2 and Cu 2p3/2 located at 962.2 and 943.6 eV further confirmed the presence of Cu^{2+} in the prepared product, suggesting the formation of amorphous CuO on the surface due to oxidation.[6]

Supplementary Note 2

A self-made glucose early warning system, consisting of a sensing module, an analysis module, and a Bluetooth module with self-developed software supporting the Android operating system, can analyze glucose levels and evaluate values timely. The self-developed software includes logical judgment statements as follows:

[{"min_num": 0, "max_num": 3.588, "msg": "Hypoglycemia", "music": " ", "flashing": 500, "emergency_user": "153****6648"},

{"min_num": 3.588, "max_num": 5.612, "msg": " Normal ", "music": " ", "flashing": 0, "emergency_user": "153****6648"},

{"min_num": 5.612, "max_num": 15, "msg": "Hyperglycemia", "music": " ", "flashing": 500, "emergency_user": "153****6648"}]

The range of values judged here is set according to the subject's specific needs. The user can personalize it by adjusting the corresponding parameters, such as the value range, alert text, warning light music, and emergency contacts, according to the actual situation of the user.

References

1. L. Wang, J. Lu, Q. Li, L. Li, E. He, Y. Jiao, T. Ye and Y. Zhang, *Adv. Funct. Mater.*, 2022, **32**, 2200922.
2. W. Tian, C. Wan, K.-T. Yong, S. Liu, S. Wei, C. Zhang, X. Liu, J. Su, W. Cheng and Y. Wu, *Adv. Funct. Mater.*, 2022, **32**, 2106958.
3. C. Dong, H. Zhong, T. Kou, J. Frenzel, G. Eggeler and Z. Zhang, *ACS Appl. Mater. Interfaces*, 2015, **7**, 20215-20223.
4. M. Wang, X. Song, B. Song, J. Liu, C. Hu, D. Wei and C.-P. Wong, *Sens. Actuators, B*, 2017, **250**, 333-341.
5. P. K. Pagare and A. P. Torane, *Microchim. Acta*, 2016, **183**, 2983-2989.
6. Y.-L. Li, Y.-H. Liu, L.-S. Chen and J.-L. Xu, *Adv. Healthcare Mater.*, 2021, **10**, 2100046.